Pergamon

Geochimica et Cosmochimica Acta, Vol. 67, No. 21, pp. 4067–4077, 2003

0016-7037/03 $30.00 + .00

doi:10.1016/S0016-7037(03)00366-1

The effects of pH, ionic strength, and iron–fulvic acid interactions on the kinetics of non-photochemical iron transformations. I. Iron(II) oxidation and iron(III) colloid formation

MICHAEL J. PULLIN[1,*] and STEPHEN E. CABANISS[2]

[1]Department of Civil Engineering and Geological Sciences, University of Notre Dame, Notre Dame, IN 46556, USA
[2]Department of Chemistry, University of New Mexico, Albuquerque, NM 87131, USA

(*Received September* 16, 2002; *accepted in revised form May* 9, 2003)

Abstract—Flow injection analysis was used to study the effect of a fulvic acid on the kinetics of iron(II) oxidation and iron colloid formation under conditions approximating fresh natural waters. While iron(II) oxidation in high-carbonate inorganic solutions is predicted well by a recently proposed homogeneous model, it overestimates the oxidation rate in low-carbonate solutions, possibly due to the formation of an intermediate iron(II) colloid or surface species. Results in fulvic acid solutions are consistent with the formation of an iron(II)–fulvic acid complex at both pH 6.0 and 8.0 which accelerates the overall oxidation rate relative to inorganic solutions. However, iron(III) complexation by fulvic acid greatly slows the formation of iron colloids, stabilizing dissolved iron(III). Decreased pH and increased ionic strength slow and decrease iron colloid formation. Evidence of a kinetic control on the distribution of iron(III) between organically complexed and colloidal forms is presented. *Copyright © 2003 Elsevier Ltd*

1. INTRODUCTION

The rates of iron(II) oxidation and iron(III) colloid formation occur on the timescale of other environmental iron reactions, including photochemical or biochemical reduction, iron hydroxide and oxide dissolution, iron-dissolved organic matter (DOM) complexation/dissociation, and biologic uptake. As a result, the kinetics of these two processes and the solution parameters that affect them, such as pH, ionic strength, and iron-ligand interactions, can have a large effect on iron cycling in natural waters. This study examines the effects of these solution parameters on iron(II) oxidation and iron colloid formation in a model freshwater system.

Numerous studies have examined the kinetics of iron(II) oxidation in homogeneous solutions containing no organic ligands (Stumm and Lee, 1961; Sung and Morgan, 1980; Millero, 1985; Millero et al., 1987, 1991; Millero and Izaguirre, 1989; King et al., 1995; King, 1998; King and Farlow, 2000). The generalized mechanism of iron(II) oxidation under these conditions is postulated to be

$$\mathrm{Fe(II)} + \mathrm{O_2} \rightleftharpoons \mathrm{Fe(III)} + \mathrm{O_2^{\bullet -}} \quad (1)$$

$$\mathrm{Fe(II)} + \mathrm{O_2^{\bullet -}} + 2\mathrm{H^+} \rightarrow \mathrm{Fe(III)} + \mathrm{H_2O_2} \quad (2)$$

$$\mathrm{Fe(II)} + \mathrm{H_2O_2} \rightarrow \mathrm{Fe(III)} + \mathrm{HO^{\bullet}} + \mathrm{HO^-} \quad (3)$$

$$\mathrm{Fe(II)} + \mathrm{HO^{\bullet}} \rightarrow \mathrm{Fe(III)} + \mathrm{HO^-} \quad (4)$$

Rate constants for Eqn. 1 and 3 and typical values of $[O_2]$ and $[H_2O_2]$ suggest that either reaction could control the rate of iron(II) oxidation, depending on conditions (Voelker and Sedlak, 1995, see Table 1). However, Emmenegger et al. (1998) found that in their O_2 saturated lake water samples, iron(II) oxidation by O_2 dominated the overall rate. Additionally, model predictions by King and Farlow (2000) suggest that O_2 oxidation will dominate the overall rate in dark, circumneutral waters, although photochemical production of H_2O_2 could make reaction 3 the rate controlling pathway in the presence of sunlight.

As noted by Eqn. 1, the back reaction of iron(III) and superoxide ($O_2^{\bullet -}$) produced during the oxidation could reduce the net oxidation rate. However, King et al. (1995) found this process did not significantly alter iron(II) oxidation rates even at low total iron concentrations, perhaps because colloidal iron(III) (the major iron[II] oxidation product at circumneutral pH) reacts much more slowly with $O_2^{\bullet -}$ than dissolved iron(III) (Voelker and Sedlak, 1995).

The exact rate of oxidation depends on the speciation of the iron(II). It has been long observed that the iron(II) oxidation rate is proportional to the square of hydroxide concentration at pH $>$ 5 (Stumm and Lee, 1961). Millero (1985) proposed that this relationship results from the relatively fast oxidation of $Fe(OH)_2^0$(aq). More recently, King presented a homogeneous iron(II) oxidation model that accounts for the effects of both iron(II) hydrolysis and iron(II)-carbonate complexation on iron(II) oxidation by O_2 and H_2O_2 (King, 1998; King and Farlow, 2000).

Naturally occurring organic ligands, such as DOM, have also been reported to affect the oxidation rate of iron(II). Theis and Singer (1973, 1974) and Miles and Brezonik (1981) reported that a variety of model iron(II)-binding ligands and humic acids decreased the rate of iron(II) oxidation. However, it has been noted that back-reduction of iron(III) oxidation products by catechol-type ligands may have decreased their observed oxidation rates (Stumm and Morgan, 1981, p. 469). In contrast, Liang et al. (1993), Voelker and Sulzberger (1996), and Emmenegger et al. (1998) all found that DOM can accelerate the iron(II) oxidation rate under some conditions. Liang et al. (1993) and Emmenegger et al. (1998) postulated that in the presence of DOM, net oxidation is the result of two competing pathways, DOM-iron(II) complexation and oxidation of the complex and oxidation of inorganic iron(II) species. Voelker

* Author to whom correspondence should be addressed (mpullin@nd.edu).

Table 1. The iron(II) oxidation model species formation constants, oxidation rate constants, and predicted contribution of each species to the overall oxidation rate.

Species	log K_f[a]	Log rate constant for oxidation by O_2[a]	Predicted % contribution of each species to the overall iron(II) oxidation rate: pH 8.0, low *I*	pH 8.0, high *I*	pH 6.0, low *I*	pH 6.0, high *I*
Fe^{2+}	n/a	–4.26	—[b]	—	—	—
$FeOH^+$	–9.51	2.62	0.8	0.8	47.7	49.3
$Fe(OH)_2$	–20.61	7.72	75.4	72.9	47.4	47.0
$FeHCO_3^+$	–6.35	<1.9	—	—	3.8[c]	2.9[c]
$FeCO_3^0$	–12.46	<1.4	1.5[c]	1.0[c]	0.9[c]	0.7[c]
$Fe(CO_3)_2^{2-}$	–28.84	5.82	8.4	11.1	—	—
$FeCO_3OH^-$	–22.17	4.0	13.9	14.2	—	—

[a] Ionic strength = 0, temperature = 25°C, taken from King (1998).
[b] <0.1% of total.
[c] Assumes that the rate constants for $FeHCO_3^+$ and $FeCO_3^0$ (aq) are equal to their maximum values.

and Sulzberger (1996) suggested that H_2O_2 oxidizes an iron(II) complex with fulvic acid more rapidly than inorganic iron(II), although Emmenegger et al. (1998) did not observe any effect of ligands on the oxidation rate by H_2O_2.

Ionic strength also affects the iron(II) oxidation rate, independent of specific iron(II)-anion interactions. In general, increasing salt concentration decreases the observed rate (Millero, 1985; Millero et al., 1987, 1991; Millero and Izaguirre, 1989; King, 1998). In dilute solutions ($I < 0.1$ mol/L), the Debye-Huckel theory predicts that the effect of an inert electrolyte on a rate constant depends only on the square root of the ionic strength (I) and the product of the charges of the reactants:

$$\log k = \log k_0 + Z_1 Z_2 I^{1/2} \quad (5)$$

where k_0 is the rate constant at $I = 0$ and Z_1 and Z_2 are the charges of two reactants (Sung and Morgan, 1980; Millero, 1985). Thus, the generally observed trend of decreased oxidation rate at increased ionic strength indicates that the positively charged iron(II) species must be reacting with a negatively charged ion (or vice-versa). However, this conflicts with the generally recognized Fe(II) oxidation mechanism presented above (Eqn. 1–4). If the charge of any species in the rate limiting step were zero (as for O_2 or H_2O_2 in the mechanism described above) then the rate should be independent of ionic strength. One explanation for this apparent disagreement is that the rate limiting step may involve the reaction of iron(II) with a charged species such as O_2OH^- (a dissociated form of hydrated molecular oxygen, O_2H_2O) and not O_2 (Kester et al., 1975; Tamura et al., 1976a; Sung and Morgan, 1980; Millero, 1985; Liang et al., 1993). However, another possibility is that increased ionic strength shifts the thermodynamically-controlled time zero iron(II) speciation to faster reacting iron(II) species.

At circumneutral pH, iron is predicted to undergo rapid hydrolysis after oxidation and form amorphous hydrous ferric oxide and/or poorly crystalline ferrihydrite, and eventually crystalline phases such as goethite, hematite, and/or lepidocrocite. While the exact nature of the iron(II) oxidation products is determined by a number of experimental (or environmental) factors, O_2 saturated conditions at near-neutral pH generally result in the eventual formation of lepidocrocite (Misawa et al., 1974; Sung and Morgan, 1980; Schwertmann and Fechter, 1994). The formation of the thermodynamically stable mineral phase can take hours to months depending on the temperature, pH, and background electrolyte composition (Schwertmann and Cornell, 1991; Cornell and Schwertmann, 1996; Schwertmann et al., 1999). For simplicity, the range of possible particulate iron(II) and iron(III) hydrolysis products will be grouped here under the general term "colloidal iron."

Particle aggregation and/or conversion of the initial amorphous iron(III) phases to more crystalline phases can be inhibited by the presence of organic ligands (Schwertmann, 1966; Cornell and Schwertmann, 1979 and 1996). Cornell and Schwertmann theorized that carboxylic and hydroxy-carboxylic acids could bind colloidal iron(III) particles into a network (Cornell and Schwertmann, 1979). Perret et al. (1994) and Taillefert et al. (2000) have published evidence of iron hydr(oxide)-organic matter networks. Previously, we have shown that the submicron filtration of natural water samples can decrease both its colloidal iron and organic carbon concentrations (Pullin, 1999; Pullin and Cabaniss, 2001). The rate and extent of colloidal iron formation in the presence in natural organic ligands has not been previously examined.

Colloidal iron formed during iron(II) oxidation may, in turn, affect the rate of further iron(II) oxidation. Studies which have examined the effect of iron (hydr)oxide surfaces on the iron(II) oxidation rate generally report that iron(II) sorption accelerates its oxidation, although only at total iron concentrations exceeding 50 μmol/L (Tamura et al., 1976b; Sung and Morgan, 1980; Wehrli, 1990). This effect is attributed to the tendency of oxygen-containing ligands, such as surface hydroxyl groups, to stabilize iron(III) over iron(II) (Luther, 1990; Luther et al., 1992).

The purpose of the research presented here is to investigate (1) the effects of fulvic acid, pH, and ionic strength on the kinetics of iron(II) oxidation, (2) the effects of initial iron redox state (iron(II) vs iron(III)), pH, and ionic strength on the kinetics of iron colloid formation in the presence of fulvic acid and (3) the interaction between the kinetics of iron(II) oxidation and iron(III) colloid formation. These topics will be explored using flow-injection analysis (FIA) and spectroscopic methods to measure iron(II) and dissolved or colloidal iron as function of time in pH and ionic strength buffered solutions with and without fulvic acid. The results will be compared to the most current homogenous inorganic iron(II) oxidation model, and extrapolated to natural systems.

2. EXPERIMENTAL

2.1. Materials

Sodium perchlorate, 3-(2-pyridyl)-5,6-diphenyl-1,2,4-triazine-*p*,*p*′-disulfonic acid (ferrozine), redistilled (99.999+%) 70% nitric acid, a 1000-μg/mL iron AA/ICP standard (1–2 wt.% HNO_3) and the hemisodium salts of 2-(N-morpholino)ethanesulfonic acid (MES) and N-(2-hydroxyethyl)piperazine-N′-(2-ethanesulfonic acid) (HEPES) were obtained from the Sigma-Aldrich Chemical Co. Suwannee River fulvic acid (SRFA) was provided by Jerry Leenheer (U.S. Geological Survey, CO). Its isolation and characterization are described elsewhere (Averett

et al., 1994). Certified ACS grade ferrous ammonium sulfate hexahydrate was obtained from Fisher Scientific. The iron(II) salt was warmed in an oven at 45°C for 1 h and stored in a desiccator until use. All other chemicals were used without additional purification or modification. High purity (≥17.8 MΩ) deionized water was used throughout.

2.2. Iron–Fulvic Acid Solution Preparation

To prepare the solutions used in the experiments, pH 6.0 (MES) or 8.0 (HEPES) buffer and SRFA were added from concentrated stock solutions to a 50 mL polypropylene volumetric flask. Experiments were conducted at two ionic strengths. For the higher ionic strength experiments, sodium perchlorate was also added to the reaction medium. In the lower ionic strength experiments, it was omitted and the ionic strength was determined mainly by the pH buffer. The solution was diluted to ~40 mL with deionized water, and mixed thoroughly. For the iron(II) oxidation experiments, iron(II) was then added from a freshly made ferrous ammonium sulfate stock solution (0.01 mol/L HNO_3). For the colloid formation experiments, iron from either the AA/ICP standard (iron[III]) or from the ferrous ammonium sulfate stock solution (iron[II]) was then added. The solution was then diluted to volume and mixed again. The measurement of either iron(II) or total dissolved iron by FIA began immediately (methodology discussed below). In a few cases, colloidal iron was measured by UV-Vis spectrophotometry, in place of the FIA analysis.

The final concentrations for all the experiments were: 10.0 mmol/L pH buffer (MES or HEPES), 10.0 mg/L fulvic acid (~5 mg C/L), 0.10 mol/L sodium perchlorate (when used), and 10.0 μmol/L iron. For the iron(II) oxidation experiments, solutions without the fulvic acid were also made and analyzed. To eliminate photochemical effects, the solution preparation and analysis were conducted in near darkness, with only the dim light from computer monitors and instrument displays present. The sample flasks were wrapped in aluminum foil once the final dilution and mixing were complete, further limiting exposure to light. Dissolved oxygen was assumed to be at saturation throughout the experiments, not unreasonable given the ~25:1 O_2:Fe ratio in these experiments and the factor of 4 in the proposed oxidation mechanism (Eqn. 1–4 and 6).

2.3. Iron–Fulvic Acid Solution Analysis

2.3.1. Iron(II) oxidation and iron colloid formation by flow injection analysis

A previously described flow injection analysis (FIA) system based on the colorimetric analysis of iron using ferrozine was used to measure total iron(II) and dissolved iron as a function of time from mixing the iron with the pH buffered solutions (Pullin, 1999; Pullin and Cabaniss, 2001). An iron(II)-specific permutation of the FIA method was used to measure iron(II) oxidation in iron–fulvic acid mixtures and control solutions without fulvic acid (Pullin and Cabaniss, 2001). Briefly, the method injects an aliquot of sample into a pH 6 buffered stream of water, which is then mixed with ferrozine. After a 25 s reaction time (at 25°C), the resulting iron(II)-ferrozine complex is then measured by absorbance at 562 nm, as a peak in time. Standardization used pH 2.0 nitric acid solutions of iron(II) from ferrous ammonium sulfate to create a linear regression between FIA peak height and iron(II) concentration. Unlike the Fe(II) chemiluminescence methods (Voelker and Sulzberger, 1996), this method is not affected by high concentrations of organic matter (Pullin and Cabaniss, 2001).

A dissolved iron FIA method was used to quantify iron colloid formation in the iron–fulvic acid mixtures as the difference between the total iron (known) and the dissolved iron (FIA measured) (Pullin and Cabaniss, 2001). Briefly, this method injects an aliquot of sample into a pH 4 buffered flowing stream of water (acetic/citric acid) which is then mixed with a reductant (ascorbic acid) and ferrozine. After a 70 s reaction time (at 65°C), the iron(II)-ferrozine complex was measured as a peak in absorbance at 562 nm in time. Standardization used pH 2.0 nitric acid solutions of iron(III) (from an AA/ICP standard) to create a linear regression between FIA peak height and iron concentration. This method was found to give good recovery of iron(III)-organic complexes, but no response to freshly made iron(III) colloids under the conditions employed here (iron[III] added to pH 6.0 and 8.0 MES and HEPES buffered solutions) (Pullin and Cabaniss, 2001). Additionally, in the analysis of a river water sample, the method was found to measure only iron passing a 0.050-μm Nuclepore (50 nm) filter (Pullin and Cabaniss, 2001). Estimates of the lower limit of aquatic colloid particle size vary from 10 to 100 nm (Perret et al., 1994; Ledin et al., 1995; Filella et al., 1997; Hassellöv et al., 1999; Taillefert et al., 2000; Vaillancourt and Balch, 2000). Clearly, either the use of a chemical reaction or a 50-nm filter as the division between colloidal and dissolved is an operational definition. However, since our FIA method gave no response to freshly made iron(III) colloids, we feel that this estimate of dissolved iron is valid under these conditions.

While the FIA analysis does not measure changes in particle size distribution during colloid formation, it does permit the fast and simple determination of the total amount of iron in the colloidal phase. This allows for the quantitative determination of the net amount of iron being transferred to the colloidal phase on a minute by minute timescale. Methods of this nature are needed to quantitatively describe the kinetics of iron colloid formation and understand the environmental parameters that control it.

2.3.2. Iron colloid formation by spectrophotometry

Iron(III) oxides and oxyhydroxides exhibit characteristic electronic absorbance spectra in the UV-visible range (Sherman and Waite, 1985). In the iron(II) oxidation experiments without fulvic acid, this absorbance was used to measure the formation of colloidal iron. This provided a faster data acquisition rate than possible using FIA. However, the overlap of the absorbance spectrum of the fulvic acid with that of the iron colloids limited the use of this method to iron solutions without fulvic acid.

To provide a quantitative measurement of the amount of iron colloids formed during these experiments, solutions containing 10.0 mmol/L pH 8.0 HEPES buffer, 0.10 mol/L sodium perchlorate, and iron concentrations of 0.50, 1.0, 3.0, 10.0, 30.0, and 50.0 μmol/L (added as iron[II]) were prepared in polypropylene flasks and allowed to stand in the dark for 60 min to allow for oxidation and colloid formation. The absorbance spectrum of each solution was collected from 300 to 600 nm in 10 cm glass cells using a Hitachi U2000 spectrometer. A 10.0-mmol/L HEPES + 0.10-mol/L sodium perchlorate solution was used in the reference cell. Using linear regression of absorbance vs. added iron concentration (Beer's law), the molar absorptivity of the colloid product (3020 M^{-1} cm^{-1}, as iron) was determined at 340 nm, a maximum above the background absorbance of the HEPES buffer (≤300 nm). This assumes that all the added iron is converted to the colloidal form, not unreasonable for micromolar pH 8.0 iron solutions with no added ligand.

To follow colloid formation over time, a 1.0 cm cell in the spectrometer reference beam was filled with 10.0 mmol/L HEPES + 0.10 mol/L sodium perchlorate pH 8.0 buffer. Fifty microliters of 50.0-μmol/L iron(II) stock solution was added to a dry 1.0-cm glass cuvette in the spectrometer sample beam followed by 2.45 mL of the 10.0-mmol/L HEPES + 0.10-mol/L sodium perchlorate pH 8.0 buffer. The sample compartment was closed and the absorbance at 340 nm was recorded every 12 s for 60 min. The absorbance vs. time data were converted to colloid concentration vs. time data using the molar absorptivity of the product determined above. The experiment was later repeated using a Hewlett Packard HP8453 diode array spectrophotometer, which collected an entire absorbance spectrum every thirty seconds for sixty minutes. No changes in the shape of the absorbance spectrum (300–400 nm) of the product over time were observed.

2.4. Iron(II) Oxidation Model Predictions

For comparison, the kinetics of iron(II) oxidation at the experimental conditions used here were predicted using a homogeneous oxidation model developed by King (1998). This model considers the oxidation of each of the iron(II) hydrolysis and carbonate species separately (Table 1). The model does not consider the effects of iron(II) complexation by organic ligands or the effect of the iron(II) oxidation product (iron[III] colloid) surface on the iron(II) oxidation rate (autocatalysis). The activities of the iron(II) species were calculated according to King (1998). Since bicarbonate was not used as a pH buffer in most of our experiments, the carbonate species were simply assumed to be in

equilibrium with the atmosphere. The hydrogen ion activity was fixed during the calculation at the value for the pH buffer used in the experiment. The oxidation rate constants for each species (Table 1) were adjusted for ionic strength using an empirical correction (King, 1998). The activities and the rate constants were used to calculate the overall iron(II) oxidation rate constant according to

$$-\frac{d[Fe(II)]}{dt} = 4[O_2]\sum_{i=1}^{n} k_i[Fe(II)X]_i \quad (6)$$

where n is the total number of species, X is the iron(II) ligand (Table 1), and k_i is the second order rate constant for the reaction of species i with O_2 (King, 1998). The $[O_2]$ at atmospheric equilibrium at 25°C was taken from the literature (Bensen and Krause, 1980). Ionic strength was assumed to have no effect on $[O_2]$ over the range examined. Because $[O_2]$ was much greater than the initial [Fe(II)] in our experiments, it was assumed to be constant over time (pseudo-first order conditions). Predicted iron(II) concentration was calculated as a function of time using the overall rate constant and the dissolved $[O_2]$.

3. RESULTS

3.1. Iron(II) Oxidation

The purposes of measuring iron(II) oxidation without any added organic ligand (Suwannee River fulvic acid—SRFA) are to provide a control to compare with the experiments containing fulvic acid and to test the homogeneous Fe(II) oxidation model of King (1998). Comparison of the measured and model predicted iron oxidation data to each other yields two important observations (Fig. 1). The first is that the King model consistently predicts faster oxidation than is observed. The second is that the experimentally measured iron(II) does not follow the expected pseudo-first order decay, especially at pH 8.0. At pH 6.0, the model predictions are in better agreement with the experimental data and the shape of the oxidation curve deviates less from the predicted first order decay (Fig. 1b). However, due to the very slow rate of oxidation at pH 6.0, the data do not extend to the completion of the oxidation reaction.

To elucidate the role of colloidal iron in the iron(II) oxidation process, we also measured its concentration by spectrophotometry (at pH 8.0 with 0.10 mol/L $NaClO_4$) (Fig. 2). The increase of colloidal iron over time confirms the non–first order behavior of the system (Fig. 2). Tadolini (1987), who also monitored the UV-Vis absorbance of the iron(III) oxidation products during the oxidation of iron(II) in pH 7.0 to 7.5 HEPES and MOPS (3-[N-morpholino]propanesulfonic acid) buffers, also reports non–first order behavior. The absorbance spectrum of the iron colloid product found in our experiments (not shown) resembles the spectra reported by Sherman and Waite (1985) for lepidocrocite and goethite.

The dissolved iron concentration during the oxidation experiment with no SRFA was calculated by subtracting the measured colloidal iron concentration from the total iron added to the experiment (Fig. 2). This dissolved iron concentration is the sum of the dissolved iron(II) and iron(III) species. Under the conditions employed in this experiment (pH 8.0, no organic ligands), where iron(III) is insoluble and its hydrolysis is very rapid, the dissolved iron(III) concentration should be near zero, making the calculated dissolved iron equal to the dissolved iron(II). However, we observed that the FIA measured iron(II) concentrations were greater than the calculated dissolved iron concentrations (Fig. 2). This "extra" measured iron(II), plotted as the difference between calculated dissolved iron and FIA measured iron(II), must be due to iron(II) associated with the colloidal phase, either as part of the colloid itself or as a sorbed surface species. The time dependence of the "colloidal iron(II)," has the characteristic shape of a reaction intermediate (Fig. 2). It should be noted that this analysis assumes that the molar absorptivity of this species is the same as the colloidal iron(III) at 340 nm, within experimental error. It also assumes that the molar absorptivity of the colloidal material does not change on the timescale of the experiment (60 min), due to changes in crystallinity or particle size. The absence of change in the shape of the oxidation product absorbance spectrum (300−400 nm) as a function of time (not shown) indicates that these assumptions are reasonable.

When we added 1.0 mmol/L total carbonate to the reaction mixture for the oxidation experiment at pH 8.0, the rate of oxidation increased so that it was in much better agreement with the model predictions (Fig. 1a). Additionally, the shape of the oxidation curve became more characteristic of first order decay (exponential), suggesting that the colloidal iron(II) intermediate species either had been eliminated or no longer controlled the oxidation rate.

We also found that the concentration of the HEPES buffer did not affect the observed oxidation rate (not shown), in agreement with the results of King (1998). Tadolini (1987) was able to show that the iron(II) oxidation product observed in both HEPES and MOPS buffers, and when iron(II) was added to unbuffered alkaline solutions, had nearly identical absorbance spectra, indicating that the increasing UV-Vis absorbance during oxidation was due to the formation of a colloidal iron(III) oxidation product, not an iron(III)-buffer complex (a possible complication here).

The addition of 10.0 mg/L SRFA to the iron(II) oxidation reaction mixture substantially increased the observed oxidation rate of iron(II) at both pH 6.0 and 8.0 (Fig. 3). Additionally, in the presence of the SRFA, the observed oxidation rate more closely resembled first order decay. At longer times, the observed oxidation rate in the presence of the fulvic acid at pH 6.0 slows, possibly approaching a steady state value (Fig. 3b).

At pH 8.0, with and without SRFA, oxidation occurs more slowly at the higher ionic strength (Figs. 1a and 3a). This is the expected trend, as noted in the introduction. Oxidation of iron(II) at pH 6.0 with no SRFA present does not conform to this trend, proceeding slightly faster at the higher ionic strength (Fig. 1b). When fulvic acid is added to the oxidation reaction at pH 6.0, the ionic strength trend returns to faster oxidation at lower ionic strength (Fig. 3b).

3.2. Colloid Formation

The addition of iron (either as Fe(II) or Fe(III)) to the pH buffered (6.0 and 8.0) SRFA solutions resulted in the formation of colloidal iron over time (Fig. 4). The rate of formation was slower at pH 6.0 than at pH 8.0. The experiments eventually reached a steady state amount of colloidal iron at long times (>48 h), except for the case of iron(II) at pH 6.0 (discussed below). The amount of steady state colloidal iron was greater at pH 8.0 than at pH 6.0. The effect of ionic strength was small (except for iron[II] at pH 6.0, discussed below), with less colloidal iron formed at the lower ionic strength.

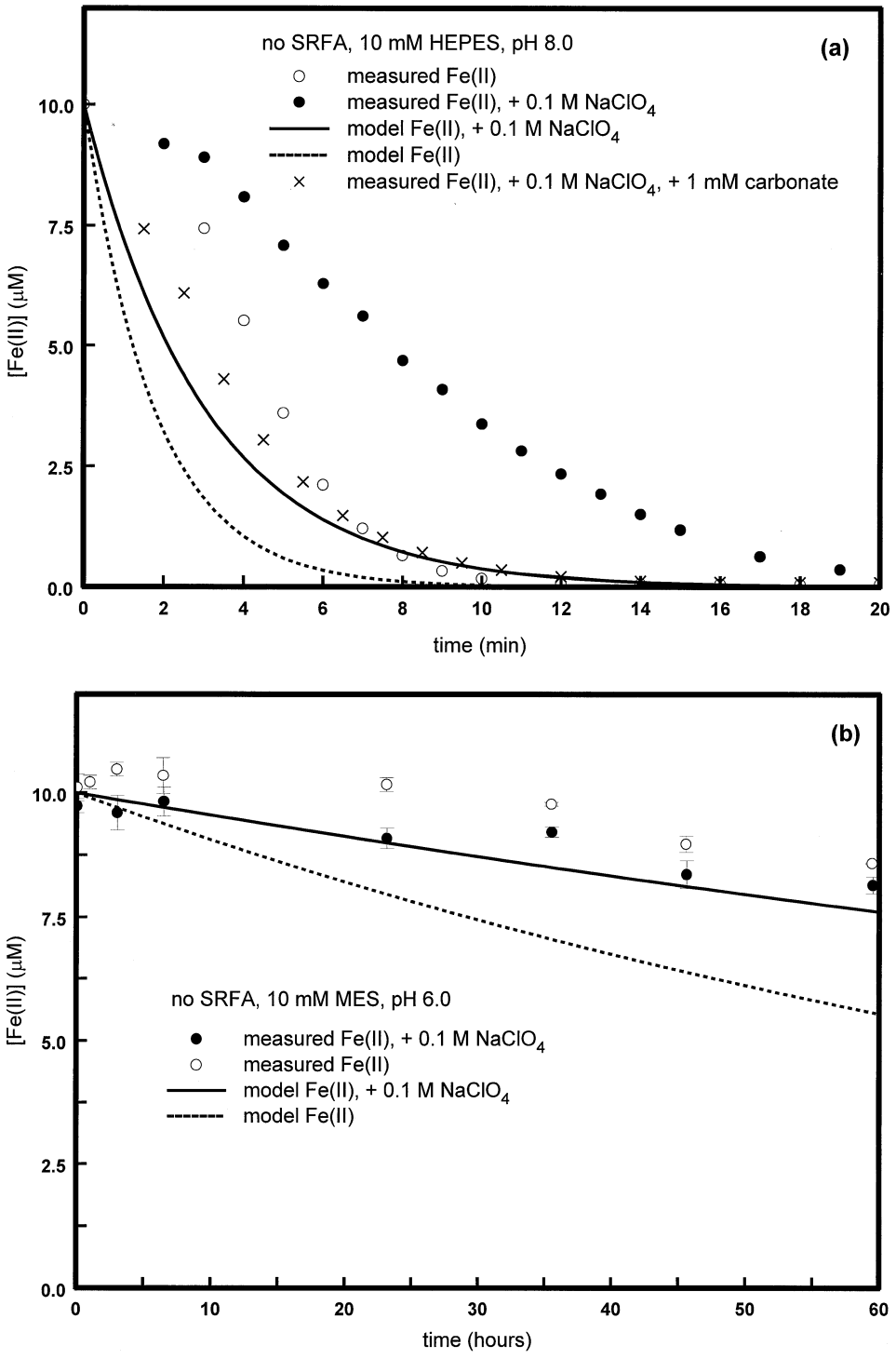

Fig. 1. Measured and modeled iron(II) oxidation in the absence of Suwannee River fulvic acid; initial [Fe(II)] = 10.0 μmol/L; pH buffer and background electrolyte indicated on the graph. Model data according to King (1998), see text for details. (a) pH 8.0, (b) pH 6.0, error bars represent $\pm 1\sigma$ of three replicate measurements.

The redox state of the iron added to start the experiment (Fe(II) vs. Fe(III)) affected the rates of iron colloid formation (Fig. 4), especially at pH 6.0 where iron(II) oxidation is relatively slow (Fig. 4b). Surprisingly, the initial iron redox state also affected the steady state amounts of colloidal iron, with experiments starting with iron(III) yielding less colloidal iron than those starting with iron(II). The pH 8.0 solutions were reanalyzed for colloidal iron after 30 d (data not shown), and the iron(II) vs. iron(III) difference was found to be stable over that time period (Pullin, 1999).

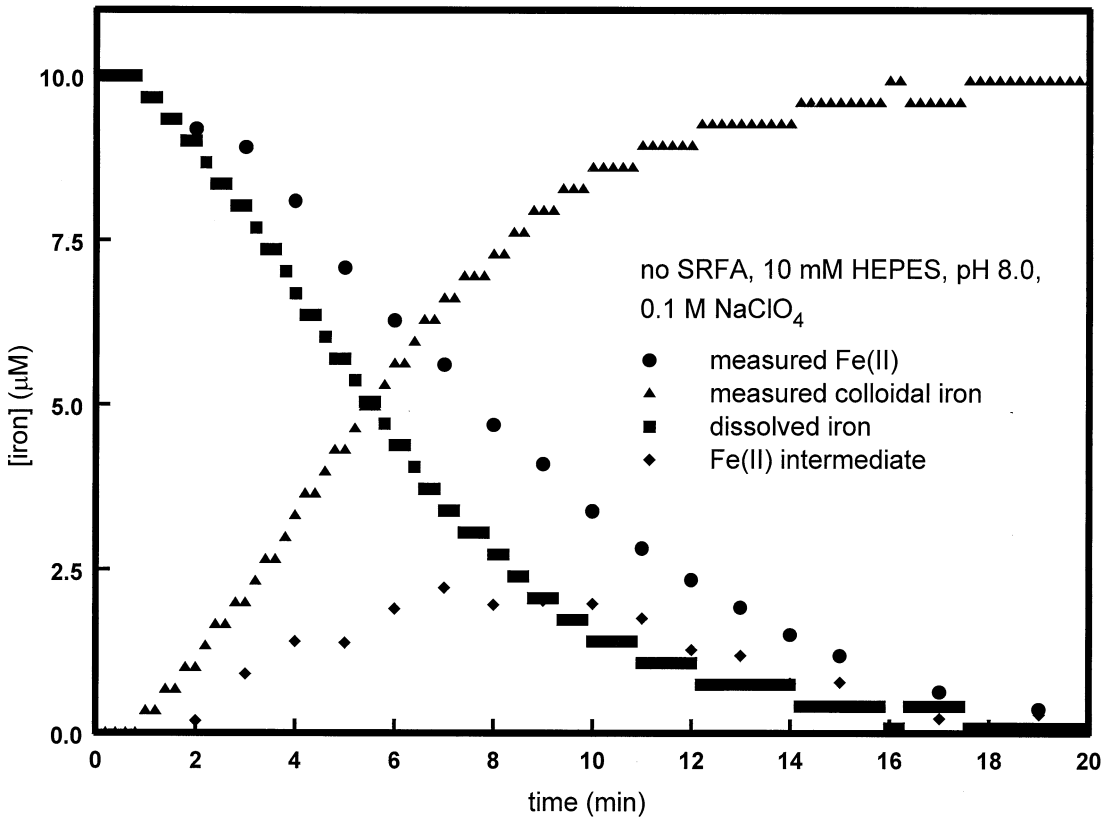

Fig. 2. The effect of autocatalysis on iron(II) oxidation; initial [Fe(II)] = 10.0 μmol/L; 10.0 mmol/L HEPES, pH 8.0; 0.10 mol/L $NaClO_4$. Iron(II) was measured by flow injection analysis and colloidal iron was measured by spectrophotometry. Dissolved iron is the difference between the total added iron and the colloidal iron. The iron(II) intermediate is the difference between the measured iron(II) and the dissolved iron.

4. DISCUSSION

4.1. Iron(II) Oxidation

The disagreement between our iron(II) oxidation data (in the absence of SRFA) and the King model may result from the inherent difficulty in determining the individual iron(II) species formation and oxidation rate constants, which could limit overall accuracy of the model predictions. However, the predicted rate constants for oxidation have expected error bounds ($\pm$0.2 log units, King, 1998) which are too small to account for the discrepancy with these experiments. A second possibility is that the rate constants for the $FeHCO_3^+$ and $FeCO_3^0$(aq) species used in the model calculations are in error. These values are only reported as upper limits by King (1998). However, examination of the predicted speciation data indicates that under our experimental conditions (atmospheric CO_2 only), the model rate of oxidation is only slightly affected by these species (Table 1).

The observation of non–first order iron(II) oxidation in the absence of SRFA suggests that a different or additional reaction mechanism (other than homogeneous oxidation) is occurring, perhaps making the model predictions an inappropriate comparison to our experimental system. In the absence of added carbonate at pH 8.0, the formation of the colloidal iron(II) intermediate appears to accelerate the oxidation rate. We interpret the observed decay curve (Fig. 1a) as initially slow oxidation (by the homogeneous mechanism) followed by fast oxidation of the intermediate. This faster reacting species is assumed to be iron(II) bound to the surface of amorphous iron(III) hydroxide particles formed during the oxidation process. This "autocatalysis" mechanism has been previously observed to accelerate iron(II) oxidation (Tamura et al., 1976b; Sung and Morgan, 1980; Wehrli, 1990), although at higher total iron concentrations ($>$50 μmol/L) than used here.

In the presence of added carbonate (Fig. 1c), carbonate out-competes the surface for the binding of iron(II) and the rate-controlling mechanism shifts to the homogeneous oxidation of iron(II)-carbonate complexes. Because the previous studies noted above used higher carbonate concentrations than employed here (as a pH buffer), the autocatalytic effect could not be observed at iron concentrations $<$ 50 μmol/L in those studies.

While the above interpretation explains the shape of the iron(II) decay curve in the absence of organic ligands, it does not resolve the disagreement between the experimental data and the model. If the colloidal iron formed during oxidation is accelerating oxidation at relatively long times, the homogeneous model (no autocatalysis) should predict a slower overall oxidation rate, roughly equal to the observed rate at short times. However, the model always predicts faster than observed rates

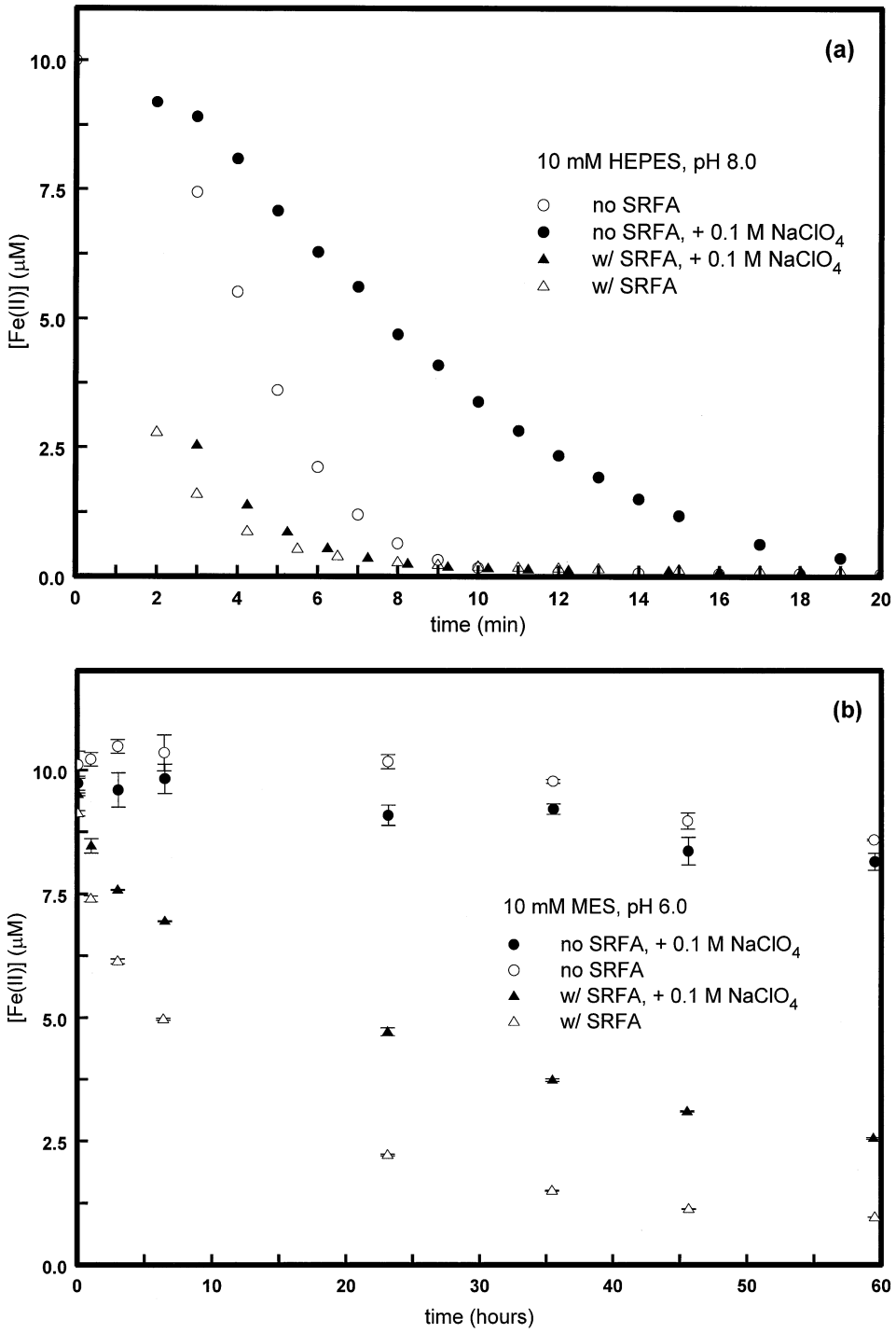

Fig. 3. The effect of Suwannee River fulvic acid on iron(II) oxidation; initial [Fe(II)] = 10.0 μmol/L; 10 mg/L fulvic acid, when used; pH buffer and background electrolyte indicated on the graph. (a) pH 8.0, (b) pH 6.0, error bars represent $\pm 1\sigma$ of three replicate measurements.

(Fig. 1). This suggests that either the oxidation rate constants for the iron(II) hydrolysis species are much smaller than previously thought, or that other less reactive iron(II) species are forming and are not accounted for by the model.

At pH 6.0 (in the absence of SRFA) the model prediction is in better agreement with the experimental data. This may be due to the reduced affinity of the iron colloid surface for iron(II) at the lower pH value. Zhang et al. (1992) have directly measured the pH dependent sorption of Fe(II) onto lepidocrocite and show increasing sorption at increasing pH (as expected for a cation) with an adsorption edge centered at ~pH 6.2. Decreased sorption could reduce the importance of the auto-

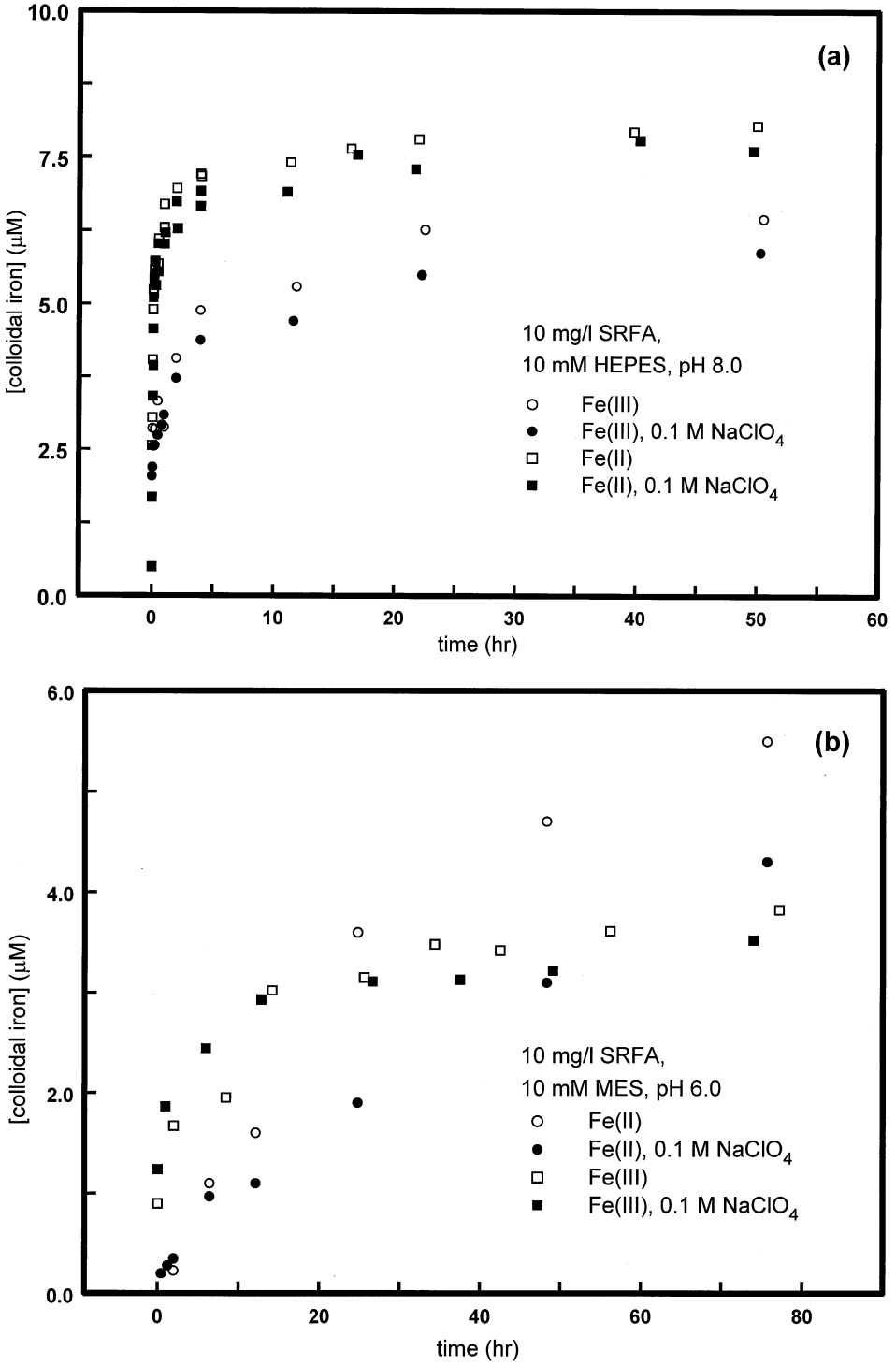

Fig. 4. The effect of pH, initial iron redox state, and ionic strength on iron(III) colloid formation in the presence of Suwannee River fulvic acid. Iron(III) colloid formation measured by flow injection analysis. 10 mg/L fulvic acid and 10.0 μmol/L total iron throughout. Labels indicate initial iron redox state, pH buffer, and background electrolyte. (a) pH 8.0, (b) pH 6.0. Note that the axes scales vary between (a) and (b).

catalytic mechanism at pH 6.0, making the homogeneous model more appropriate.

The presence of SRFA greatly increased the rate of oxidation at both pH values (6.0 and 8.0) (Fig. 3). This suggests that a relatively fast reacting iron(II)–fulvic acid complex formed, providing a faster pathway for oxidation than the surface catalyzed oxidation mechanism observed in its absence, thereby shifting the control of the oxidation rate to a homogeneous

process. Complexation of the iron(III) produced during the oxidation reaction would also decrease the amount of colloidal iron, reducing its effect on iron(II) oxidation. Additionally, SRFA sorption to the surface of colloidal iron may have prevented the formation of the colloidal iron(II) intermediate seen in the non–fulvic acid system (although decreased sorption is expected at pH 8.0 relative to pH 6.0).

However, elimination or modification of the colloidal iron phase by the fulvic acid cannot be the *only* reason for the observed shift in iron(II) oxidation kinetics. If this were true, the oxidation rate in the presence of the fulvic acid would be slower overall and equal to the rate observed at short times in the non–fulvic acid experiments. Thus, these results demonstrate that in the presence of fulvic acid, an iron(II)–fulvic acid complex forms and controls the oxidation rate at both pH 6.0 and 8.0.

The observation of an iron(II)–fulvic acid complex at saturated dissolved oxygen concentrations seems to disagree with the conclusion of Liang et al. (1993) that these conditions prevent its formation. However, their results were obtained at a lower fulvic acid concentration ($\leq$2.0 mg/L) than ours (10.0 mg/L), perhaps decreasing the iron(II) complexation effect. When their oxidation experiments were conducted at lower than saturated O_2 values, iron(II)–fulvic acid complex formation and subsequent oxidation was faster than inorganic dissolved iron(II) species hydrolysis and oxidation. Our results are consistent with the report of Emmenegger et al. (1998), who noted the acceleration of the oxidation rate, relative to model predicted values in the absence of complexation, at pH values < 7.3. Thus, conditions that favor organic complexation (such as increased fulvic acid concentration) or conditions that slow oxidation of the inorganic iron(II) species relative to iron(II)-DOM complexes (such as decreased pH) will favor control of the oxidation rate by the oxidation of iron(II) organic complexes.

It should be noted that Emmenegger et al. (1998) worked at much lower initial iron(II) concentrations (30 nmol/L) than this study (10 μmol/L), although at similar DOC concentrations (3.2 mg/L vs. $\sim$5 mg/L). One might predict that complexation would have a larger effect at a lower metal to ligand ratio (more complete complexation of the metal), but this does not seem to be borne out experimentally. A small amount of a relatively fast-reacting iron(II) complex could have a large effect on the overall oxidation rate, even if the complex is only a small percentage of the total iron(II).

It should also be noted that Emmenegger et al. (1998) conducted their experiments with unfiltered natural water samples. However, in their experiments, 0.45-μm filtration was not able to remove *all* of the accelerating effect of ligands (colloids, bacteria, or otherwise). The results presented here support their conclusion (based on their large and non-catalytic concentration of iron[II]-binding ligand), that their observed acceleration was due to the presence of "unspecific organic ligands."

The apparent decrease in oxidation rate at long times at pH 6.0 in the presence of SRFA (Fig. 3b) could be due to the back reaction of iron(III) with superoxide (reverse of Eqn. 1). However, both further reaction with additional iron(II) (Eqn. 2) and organic matter-catalyzed decomposition (Goldstone and Voelker, 2000) should rapidly remove superoxide from solution. It is more likely that the "dark" or thermal reduction of iron(III) by fulvic acid could eventually decrease the net rate of oxidation, leading to the observed non-zero iron(II)concentration at long times (Fig. 3b). The lack of net iron(II) dark reduction at pH 8.0 may simply be due to its much faster rate of oxidation at this pH value and does not necessarily imply a strong pH dependence for thermal reduction. Quantifying the effect this thermal reduction on the iron speciation is the subject of a companion publication (Pullin and Cabaniss, 2003).

The observation here of both iron(II) complexation and iron(III) chemical reduction by DOM may explain why Theis and Singer (1973, 1974) and Miles and Brezonik (1981) observed that several humic acids and some model ligands slowed or inhibited the rate of iron(II) oxidation. Thermal reduction may have substantially decreased their net rates of oxidation (Stumm and Morgan, 1981, p. 469). Experimental evidence for iron(III) reduction by ligands similar to their model compounds is now available (Lau et al., 1989; Moran et al., 1997; Lopes et al., 1999).

To summarize, the dominant oxidation mechanism for Fe(II) changes with solution conditions. Low pH and high DOC favor control of the oxidation process by Fe(II)-organic complex(es). High pH and/or high carbonate concentration favor control of the rate by iron(II)-carbonate or hydroxide species. Additionally, the autocatalytic effect can be important at lower iron(II) concentrations than previously thought, depending on the presence of iron(II) ligands in solution (carbonate or otherwise). It is clear from our data that iron(II)-organic complexes can both form and control the iron(II) oxidation rate under conditions similar to those present in a variety of surface waters (5 mg/L DOC, pH 6–8, saturated O_2). Efforts to quantitatively model iron(II) dynamics in these waters will need to account for the effect iron(II) complexation, both at mineral surfaces and in solution by inorganic and/or organic ligands.

4.2. Colloid Formation

In the presence of the fulvic acid, the iron remaining in the dissolved phase after colloid formation greatly exceeds the predicted solubility of iron(III) in its absence (Fig. 4), presumably due to complexation by the fulvic acid. The observed rate of iron colloid formation is also much slower than would be expected in the absence of SRFA. For example, in the iron(II) oxidation experiment at pH 8.0 without SRFA, the colloidal iron concentration reached $\sim$100% of the total added iron within 15 min (Fig. 2).

The increased amount of colloid formation at pH 8.0, relative to pH 6.0, is presumably due to increased iron(III) hydrolysis. The effect of this increased hydrolysis must at least partially offset the increased metal complexation by SRFA at the higher pH. At pH 6.0, the colloid formation is faster when starting with iron(III) than with iron(II) (Fig. 4b), due to the high solubility and slow oxidation rate of iron(II) at that pH. At pH 8.0, due to the relatively rapid rates of both iron(III) hydrolysis and iron(II) oxidation, the rate of colloid formation is similar when starting with iron(II) or iron(III) and is much faster than at pH 6.0 (Fig. 4).)

The small effect of ionic strength on the colloid formation rates and steady state amounts suggests that the observed rate is not due to the coagulation of smaller particles, which is en-

hanced by increased electrolyte concentrations through the partial neutralization of repulsive charges (Stumm and Morgan, 1981). The net removal of dissolved iron to the suspended colloid phase is thus limited by reaction of a dissolved Fe species, e.g., Fe(II) oxidation or Fe sorption onto a colloid. This would be consistent with decreased colloid formation at higher ionic strength, as an increased electrolyte concentration would decrease the activity of the reacting species.

When the oxidation rate of iron(II) controls the rate of colloid formation, any effect of ionic strength on the oxidation rate will also influence the colloid formation rate. In SRFA solution at pH 6.0, faster oxidation at the lower ionic strength is consistent with faster colloid formation under these conditions (Fig. 4). In SRFA solution at pH 8.0, the ionic strength effect on the colloid formation rate is smaller, as would be predicted from the short half life of iron(II) and the consequent decreased effect of the oxidation rate.

As noted above, the overall colloid formation at long times is greater at both pH values when starting with iron(II), relative to starting with iron(III) (Fig. 4). This difference must result from the kinetic control of the distribution of species, as a thermodynamic consideration would predict no difference at long times. This complex kinetic behavior could result from multiple pathways to the formation of colloidal iron, which would suggest the presence of multiple classes of iron–fulvic acid complexes. It is clear from these experiments that both iron(II) and iron(III) fulvic acid complexes exist. The kinetic evidence suggests that the iron(II) complexes are fast reacting, while the iron(III) complexes are far more stable. Given the nature of iron(III) hydrolysis and fulvic acid heterogeneity, multiple iron(III) complexes or classes of complexes appear likely. While this argument is speculative, further evidence for multiple iron(III)–fulvic acid complexes is given in the companion publication (Pullin and Cabaniss, 2003).

These results also suggest that environmental processes that cause the production of iron(II) (such as photochemical reduction) may eventually promote the formation of colloidal iron. For example, several researchers have reported the photochemical production of iron colloids in humic and iron-rich waters (Gao and Zepp, 1998; Maurice et al., 2002). Gao and Zepp (1998) hypothesized that this observation was the result of photochemical destruction of the iron-binding capacity of the DOM, decreasing the solubility of the iron. While mechanisms for the iron-catalyzed photochemical decarboxylation of DOM have been proposed (Faust and Zepp, 1993; Faust, 1994), we speculate that the photoreduction of iron(III) to iron(II), followed by increased colloid formation, may be an additional mechanism causing this phenomenon.

5. CONCLUSIONS

1. In the absence of organic ligands, experimentally measured rates of iron(II) oxidation were significantly slower than predicted by the homogeneous oxidation model of King (1998). While both dissolved iron(II) and colloidal iron measurements indicate the presence of a rate-controlling autocatalytic oxidation mechanism in these experiments, it does not account for the observed systematic error in the model predictions.
2. In the presence of Suwannee River fulvic acid, kinetic evidence indicates that an iron(II)-organic complex forms over the pH range 6.0 to 8.0. These results suggest that such complexes can control the rate of iron(II) oxidation and that, in addition to the H^+, O_2, and carbonate concentrations, the concentration of DOM is an important variable controlling the rates and significance of this mechanism in natural waters.
3. SRFA slows the rate and decreases the formation of iron(III) colloids, presumably by stabilizing non-colloidal iron through complexation. Due to increased iron(III) hydrolysis and faster iron(II) oxidation, higher pH values lead to faster and more extensive colloid formation. Over the range explored here, increased ionic strength slows the rate and decreases colloid formation.
4. The distribution of iron between multiple dissolved iron(II) and iron(III)–fulvic acid complexes and colloidal iron is kinetically controlled over the time scale of these experiments (up to 30 d).

Acknowledgments—D. Whitney King (Colby College) generously provided the model iron(II) oxidation rate constants used here. Jerry Leenheer (USGS) for provided the Suwannee River fulvic acid. The authors also wish to thank Bettina Voelker (MIT), the associate editor, and several anonymous reviewers for helpful comments on the manuscript. This research was funded by the National Science Foundation (EAR-9628461).

Associate editor: C. M. Eggleston

REFERENCES

Averett R. C., Leenheer J. A., McKnight D. M., and Thorn K. A., eds. (1994) *Humic Substances in the Suwannee River, Georgia: Interactions, Properties, and Proposed Structures*. U.S. Geological Survey Water Supply Paper 2373, U.S. Government Printing Office.

Bensen B. B. and Krause D. Jr. (1980) The concentration and isotopic fractionation of gases dissolved in freshwater in equilibrium with the atmosphere. 1. Oxygen. *Limnol. Oceanogr.* **25**, 662–671.

Cornell R. M. and Schwertmann U. (1979) Influence of organic anions on the crystallization of ferrihydrite. *Clays and Clay Mineral.* **27**, 402–410.

Cornell R. M. and Schwertmann U. (1996) The Iron Oxides: Structure, Properties, Reactions, Occurrence, and Uses. VCH, New York.

Emmengger L., King D. W., Sigg L., and Sulzberger B. (1998) Oxidation kinetics of Fe(II) in a eutrophic Swiss lake. *Environ. Sci. Technol.* **32**, 2990–2996.

Faust B. C. (1994) A review of the photochemical redox reactions of iron(III) species in atmospheric, oceanic, and surface waters: Influences on geochemical cycles and oxidant formation. In *Aquatic and Surface Photochemistry* (eds. G. R. Helz, R. G. Zepp, and D. G. Crosby), pp. 3–39. Lewis Publishers.

Faust B. C. and Zepp R. G. (1994) Photochemistry of aqueous iron(III) polycarboxylate complexes, roles in the chemistry of atmospheric and surface waters. *Environ. Sci. Technol.* **27**, 2517–2522.

Filella M., Zhang J., Newma M. E., and Buffle J. (1997) Analytical applications of photo correlation spectroscopy for size distribution measurements of natural colloidal suspensions: Capabilities and limitations. *Colloids Surf. A* **120**, 27–46.

Gao H. and Zepp R. G. (1998) Factors influencing photoreactions of dissolved organic matter in a coastal river of the southeastern United States. *Environ. Sci. Technol.* **32**, 2940–2946.

Goldstone J. V. and Voelker B. M. (2000) Chemistry of superoxide radical in seawater: CDOM associated sink of superoxide in coastal waters. *Environ. Sci. Technol.* **34**, 1043–1048.

Hassellöv M., Lyvén B., Haraldsson C., and Sirinawin W. (1999) Determination of continuous size and trace element distribution of colloidal material in natural waters by on-line coupling of flow field-flow fractionation with ICP-MS. *Anal. Chem.* **71**, 3497–3502.

Kester D. R., Byrne R. H., and Liang Y. (1975) Redox reactions and solution complexes of iron in marine systems. In *Marine chemistry*

in the Coastal Environment, ACS Symposium Series 18 (ed. T. M. Church), pp. 56–79. American Chemical Society.

King D. W. (1998) Role of carbonate speciation on the oxidation rate of Fe(II) in aquatic systems. *Environ. Sci. Technol.* **32**, 2997–3003.

King D. W. and Farlow R. (2000) Role of carbonate speciation on the oxidation of Fe(II) by H_2O_2. *Mar. Chem.* **70**, 201–209.

King D. W., Lounsbury H. A., and Millero F. J. (1995) Rates and mechanism of Fe(II) oxidation at nanomolar total iron concentrations. *Environ. Sci. Technol.* **29**, 818–824.

Lau O., Luk S., and Huang H. (1989) Spectrophotometric determination of tannins in tea and beer samples with iron(III) and 1,10-phenanthroline as reagents. *Analyst* **114**, 631–633.

Ledin A., Karlsson S., Duker A., and Allard B. (1995) Characterization of the submicrometer phase in surface waters—A review. *Analyst* **120**, 603–608.

Liang L., McNabb J. A., Paulk J. M., Gu B., and McCarthy J. F. (1993) Kinetics of Fe(II) oxidation at low partial pressures of oxygen in the presence of natural organic matter. *Environ. Sci. Technol.* **27**, 1864–1870.

Lopes G. K. B., Schulman H. M., and Hermes-Lima M. (1999) Polyphenol tannic acid inhibits radical formation from Fenton reaction by complexing ferrous ions. *Biochim. Biophys. Acta* **1472**, 142–152.

Luther G. W., III (1990) The frontier-molecular-orbital approach in geochemical processes. In *Aquatic Chemical Kinetics: Reaction Rates of Processes in Natural Waters* (ed. W. Stumm), pp. 173–198. Wiley-Interscience, New York.

Luther G. W., III, Kostka J. E., Church T. M., Sulzberger B., and Stumm W. (1992) Seasonal iron cycling in the salt-marsh sedimentary environment: The importance of ligand complexes with Fe(II) and Fe(III) in the dissolution of Fe(III) minerals and pyrite, respectively. *Mar. Chem.* **40**, 81–103.

Maurice P. A., Cabaniss S. E., Drummond J., and Ito E. (2002) Hydrogeochemical controls on the variations in chemical characteristics of natural organic matter at a small freshwater wetland. *Chem. Geol.* **187**, 59–77.

Miles C. J. and Brezonik P. L. (1981) Oxygen consumption in humic-colored waters by a photochemical ferrous-ferric catalytic cycle. *Environ. Sci. Technol.* **15**, 1088–1095.

Millero F. J. (1985) The effect of ionic interactions on the oxidation of metals in natural waters. *Geochim. Cosmochim. Acta* **49**, 547–553.

Millero F. J. and Izaguirre M. (1989) Effect of ionic strength and ionic interactions on the oxidation of Fe(II). *J. Solut. Chem.* **18**, 585–599.

Millero F. J., Sotolongo S., and Izaguirre M. (1987) The oxidation kinetics of Fe(II) in seawater. *Geochim. Cosmochim. Acta* **51**, 793–801.

Millero F. J., Sotolongo S., Stade D. J., and Vega C. A. (1991) Effect of ionic interactions on the oxidation of Fe(II) with H_2O_2 in aqueous solutions. *J. Solut. Chem.* **20**, 1079–1092.

Misawa T., Hashimoto K., and Shimodaira S. (1974) The mechanism of formation of iron oxide and oxyhydroxides in aqueous solutions at room temperature. *Corrosion Sci.* **14**, 131–149.

Moran J. F., Klucas R. V., Grayer R. J., Abian J., and Becana M. (1997) Complexes of iron with phenolic compounds from soybean nodules and other legume tissues: Peroxidant and antioxidant properties. *Free Radical Biol. Med.* **22**, 861–870.

Perret D., Newman M. E., Negre J. C., Chen Y. W., and Buffle J. (1994) Submicron particles in the Rhine River—I. Physico-chemical characterization. *Water Res.* **28**, 91–106.

Perret D., Newman M. E., Negre J. C., Chen Y. W., and Buffle J. (1994) Submicron particles in the Rhine River—II. Comparison of field observations and model predictions. *Water Res.* **28**, 107–118.

Pullin M. J. (1999) *The Thermodynamics and Kinetics of Iron-Dissolved Organic Matter Interactions in Model Fresh Waters*. Ph.D. dissertation, Kent State University.

Pullin M. J. and Cabaniss S. E. (2001) Colorimetric flow-injection analysis of dissolved iron(II) and total iron in natural waters containing dissolved organic matter. *Water Res.* **35**, 363–372.

Pullin M. J. and Cabaniss S. E. (2003) The effects of pH, ionic strength, and iron–fulvic acid interactions on the kinetics of non-photochemical iron transformations. II. The kinetics of complexation and thermal reduction. *Geochim. Cosmochim. Acta* **63**, 0000–0000.

Schwertmann U. (1966) Inhibitory effect of soil organic matter on the crystallization of amorphous ferric hydroxide. *Nature* **212**, 645–646.

Schwertmann U. and Cornell R. M. (1991) Iron Oxides in the Laboratory: Preparation and Characterization. VCH, New York.

Schwertmann U. and Fechter H. (1994) The formation of green rust and its transformation to lepidocrocite. *Clay Miner.* **29**, 87–92.

Schwertmann U., Friedl J., and Stanjek H. (1999) From Fe(III) ions to ferrihydrite and then to hematite. *J. Colloid Interface Sci.* **209**, 215–223.

Sherman D. M. and Waite T. D. (1985) Electronic spectra of Fe^{3+} oxides and oxide hydroxides in the near IR to near UV. *Am. Mineral.* **70**, 1262–1269.

Stumm W. and Lee G. F. (1961) Oxygenation of ferrous iron. *Industr. Eng. Chem.* **53**, 143–146.

Stumm W. and Morgan J. J. (1981) Aquatic Chemistry: An Introduction Emphasizing Chemical Equilibria in Natural Waters. John Wiley, New York.

Sung W. and Morgan J. J. (1980) Kinetics and product of ferrous iron oxygenation in aqueous systems. *Environ. Sci. Technol.* **14**, 561–568.

Tadolini B. (1987) Iron autoxidation in MOPS and HEPES buffers. *Free Radical Res. Commun.* **4**, 149–160.

Taillefert M., Lienemann C. P., Gaillard J. F., and Perret D. (2000) Speciation, reactivity, and cycling of Fe and Pb in a meromictic lake. *Geochim. Cosmochim. Acta* **64**, 169–183.

Tamura H., Goto K., and Nagayama M. (1976a) Effect of anions on the oxygenation of ferrous ions in neutral solutions. *J. Inorg. Nucl. Chem.* **38**, 113–117.

Tamura H., Goto K., and Nagayama M. (1976b) The effect of ferric hydroxide on the oxygenation of ferrous ions in neutral solutions. *Corrosion Sci.* **16**, 197–207.

Theis T. L. and Singer P. C. (1973) The stabilization of ferrous iron by organic compounds in natural waters. In *Trace Metals and Metal-Organic Interactions in Natural Waters* (ed. P. C. Singer), pp. 303–320. Ann Arbor Science Publishers Inc., Ann Arbor, MI..

Theis T. L. and Singer P. C. (1974) Complexation of iron(II) by organic matter and its effect on iron(II) oxygenation. *Environ. Sci. Technol.* **8**, 569–573.

Vaillancourt R. D. and Balch W. M. (2000) Size distribution of marine submicron particles determined by flow field-flow fractionation. *Limnol. Oceanogr.* **45**, 485–492.

Voelker B. M. and Sedlak D. L. (1995) Iron reduction by photoproduced superoxide in seawater. *Mar. Chem.* **50**, 93–102.

Voelker B. M. and Sulzberger B. (1996) Effects of fulvic acid on Fe(II) oxidation by hydrogen peroxide. *Environ. Sci. Technol.* **30**, 1106–1114.

Wehrli B. (1990) Redox reactions of metal ions at mineral surfaces. In *Aquatic Chemical Kinetics: Reaction Rates of Processes in Natural Waters* (ed. W. Stumm), pp. 311–336. Wiley-Interscience, New York.

Zhang Y., Charlet L., and Schindler P. W. (1992) Adsorption of protons, Fe(II) and Al(III) on lepidocrocite (γ-FeOOH). *Colloids Surf.* **63**, 259–268.